# STUDY OF AN ORDER TWO DPCM TRANSMISSION SYSTEM WITH ZERO INPUT.

Danièle Fournier-Prunaret

*GESNLA-LESIA, DGEI, INSA, 135 avenue de Rangueil, 31077 Toulouse, France*, daniele.fournier@insa-tlse.fr

**Abstract : This paper deals with problems of Differential Pulse Code Modulation (DPCM) transmission system. It includes an encoder which uses a coupling between a transversal predictor and a non-linear quantifier. Many studies have been done about this model ([1][3][4]). The study is done here with a zero input in the system. It makes appear the intrinsic properties of the modulator, putting in evidence phenomena due to the quantization noise. The system is studied with the tools of non linear dynamics (study of bifurcations in the parameter plane, evolution of the stability of the system when considering attractors, basin of attractors,…). Specific symmetry properties are put in evidence. The study is completed with frequency studies of output signal, when chaotic phenomena occur.**

## I INTRODUCTION

The considered system is a *DPCM* (*Differential Pulse Code Modulation*) transmission. It includes an encoder which uses a coupling between a transversal predictor and a non-linear quantifier. The quantifier characteristic, $Q(e)$, is non-linear and bounded. The predictor, in this paper, is supposed to be of order 2. The order 1 case has been studied in [1]. The encoder is depicted in Figure1 (see [1] for details):

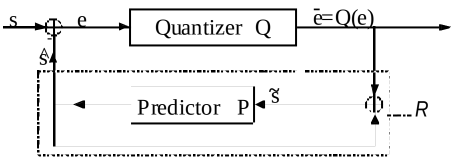


**Figure 1**: DPCM system encoder

The encoder output signal at time n+1 is: (1)

$$\hat{s}_{n+1} = a_1\hat{s}_n + a_1\, Q(s_n - \hat{s}_n) + a_2\hat{s}_{n-1} + a_2\, Q(s_{n-1} - \hat{s}_{n-1})$$

where $a_1$, $a_2$ are prediction factors and $s_n$ is the amplitude of input signal (here, $s_n$ is chosen constant equal to 0). Let $x_n \equiv \hat{s}_{n-1}$, $y_n \equiv \hat{s}_n$, then one has:

$$(2)\begin{cases} x_{n+1} = y_n, \\ y_{n+1} = a_1(y_n + Q(-y_n)) + a_2(x_n + Q(-x_n)) \end{cases}$$

which is the encoder modelisation, (2) corresponds to the equation of a two-dimensional non-invertible map $T(x_n, y_n)$. The quantifier characteristic is chosen as follows:

$$(2a)\ Q(e) = \tanh(pe)\ ,$$

$p$ is the quantifier compression gain ($p>1$; in this paper, $p = 10$ or $p = 100$). So, the map (2) depends on three real parameters ($a_1, a_2, p$).

The following symmetry property can be remarked :

$$T(-x, -y) = -T(x, y) \qquad (2b)$$

## II CRITICAL LINES

An important tool used to study non-invertible maps is that of critical curves, which has been introduced by Mira (see [2] for more details). A non-invertible map is characterized by the fact that a point in the phase plane can possess different number of rank-1 preimages, depending where it is located in the phase plane.

A *critical curve LC* is the geometrical locus, in the phase plane, of points $X$ having two coincident preimages, $T^{-1}(X)$, located on a curve $LC_{-1}$. It is recalled that the set of points $T^{-n}(X)$ constitutes *the rank-n preimages* of a given point $X$. The curve $LC$ verifies $T^{-1}(LC) \supseteq LC_{-1}$ or $T(LC_{-1}) = LC$ and separates the phase plane in two regions where each point has a different number of preimages ($k$ in one region and $k$+2 in the other one, $k \in$ N).

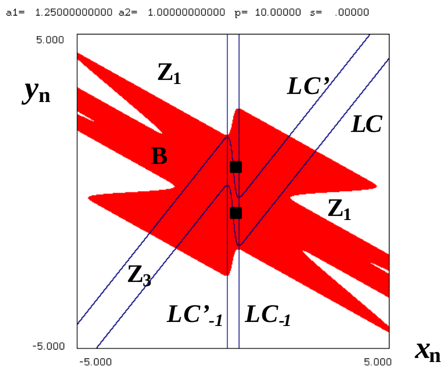


**Figure 2**: In the phase plane, basin of an attractive order 2 cycle (small black squares). Each point of the $Z_3$ area has 3 preimages. The basin of the order 2 cycle is connected.

For the map (2), one defines:

$$(3)\begin{cases} LC_{-1} : x = -\dfrac{q}{p} \\ \\ LC'_{-1} : x = +\dfrac{q}{p} \quad où \quad p \equiv \cosh^2 q \end{cases}$$

and the critical curves $LC$ and $LC'$ by:

$$(4)\begin{cases} LC: y = a_1(x+\tanh p(-x)) + a_2 a \\ \quad where\ a \equiv \tanh q - \dfrac{q}{p} \\ LC': y = a_1(x+\tanh p(-x)) + a_2 a \end{cases}$$

The curves *LC* and *LC'* separate the phase plane in three regions $Z_1$, $Z_3$, $Z_1$ (cf. Fig. 2). In $Z_1$, each point of the phase plane has one rank-1 preimage. Inside $Z_3$, each point has three rank-1 preimages. For fixed parameter values, it is possible to define in the phase plane the *basin* of an attractor, that means the set of initial conditions giving rise to iterated sequences converging towards the considered attractor. The Figure 2 shows the basin B of an order 2 attractive cycle.

## III PARAMETER PLANE

Figures 3 and 4 represent the parameter plane $(a_1, a_2)$ when $p$ is fixed. In Figures 3 and 4, one can see the regions of parameter plane $(a_1, a_2)$ where at least a periodic orbit of order k exists (k=1,2,…,14). The black region (k=15) corresponds to the existence of bounded iterated sequences, the white region to existence of divergent iterated sequences. One can recognize on the figure period doubling bifurcations, Neïmark-Sacker bifurcations with Arnold's tongues structure [3].

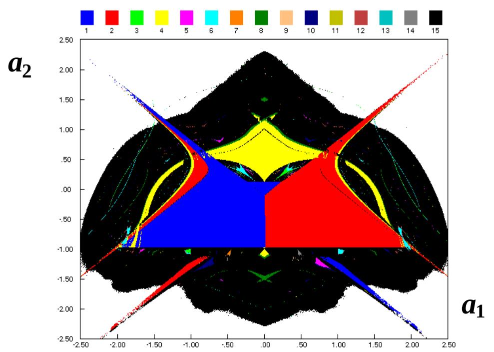


**Figure 3**: Parameter plane $(a_1, a_2)$ when $p$=10.

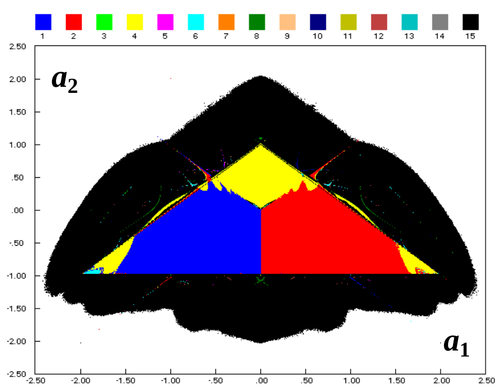


**Figure 4**: Parameter plane $(a_1, a_2)$ when $p$=100.

## IV STUDY OF CHAOTIC SETS

Figures 5a-6a-7a-8a represent ,in the phase plane $(x, y)$, chaotic attractors and their basin for different parameter values ($p$ = 10). The evolution of attractors and their basin is given and explained directly in Figures. Some of the bifurcations, which are described in this paper, have been obtained in different ways and are better explained in [2][3][4][5].

We are also interested by frequency studies. To describe the spectral components of a chaotic signal, we consider the sequence $x_n$ as one realization of a stationary discrete random process, and we estimate the Power Spectral Density (PSD) of the process, using the non-parametric Welch's method (averaged periodograms of windowed signal sections). And, when we restrict initial conditions to the basin of a single attractor, it seems reasonable to assume that the process is stationary. So, in Figures 5b-6b-7b-8b, the plot of the estimated real-valued PSD shows the spectrum of $x_n$, at positive frequencies only (since $x_n$ is always real), in decibels, versus normalized frequency.

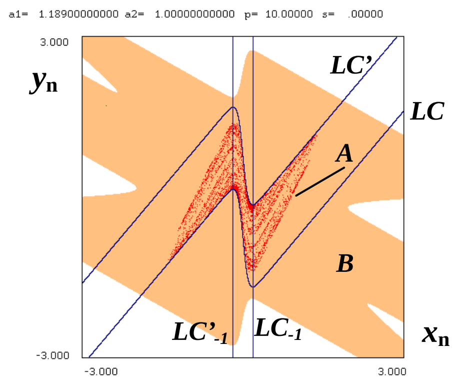


**Figure 5a**: Chaotic attractor A and its basin B. This attractor is issued from a classical period doubling bifurcation cascad giving rise to chaos.

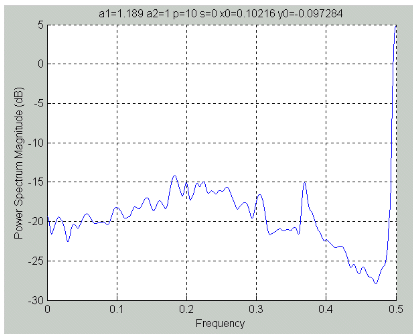


**Figure 5b**: PSD of the chaotic attractor A of Figure 5a. One recognizes a peak at the frequency 1/2, related to the cascad of bifurcations (period doubling) which gives rise to the chaotic attractor of Figure 5a [5].

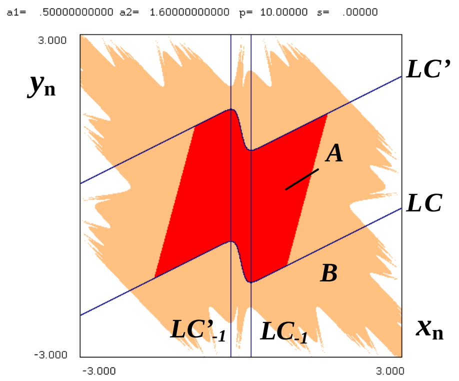


**Figure 6a**: Chaotic attractor A and its basin B. The size of A has increased.

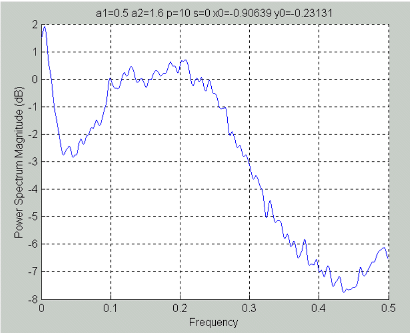


**Figure 6b**: PSD of the chaotic attractor A of Figure 6a. The peak at frequency 0.5 has disappeared.

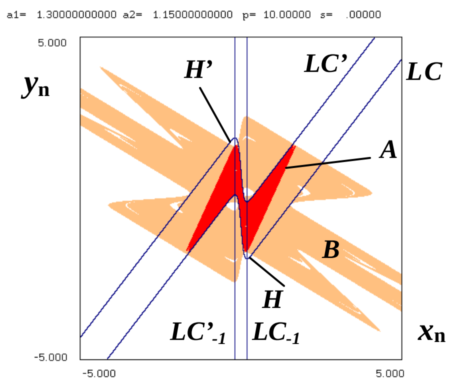


**Figure 7a**: Chaotic attractor A and its basin B. Holes have appeared inside B, due to the crossing of the basin boundary through critical lines LC and LC'. Holes are the preimages of any rank of domains H and H'.

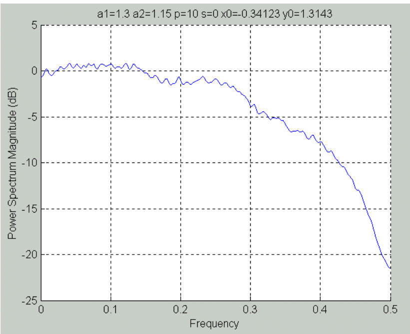


**Figure 7b**: PSD of the chaotic attractor A of Figure 7a.

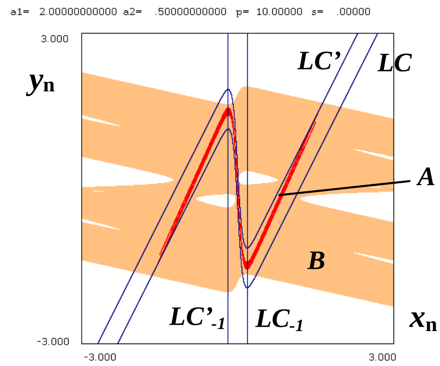


**Figure 8a**: Chaotic attractor A and its basin B with holes.

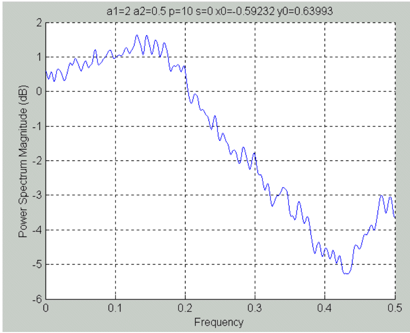


**Figure 8b**: PSD of the chaotic attractor A of Figure 8a. The spectrum is more noisy than in Figure 7b.

In Figures 7a and 8a, the chaotic attractor is very close to the bifurcation which gives rise to its destruction : contact bifurcation between itself and its basin boundary [2][3][4]. No specific periodic component appears in the spectrum.

## V STUDY OF CHAOTIC SETS – A1=0

Figures 9a, 9b, 10a show chaotic sets in the phase plane when $a_1 = 0$ ($p = 10$ or $p = 100$). In this case, the critical curves (4) become straight lines and their images and preimages also. It has been shown in [6] that segments of critical curves and their images limit absorbing areas in the phase plane; this is the case on Figure 9a, a square limited by segments of LC and LC' and their images $LC_1$ and $LC'_1$ is absorbing, this square contains a chaotic attractor, whose basin is given on Figure 9a and an invariant chaotic set of zero Lebesgue measure (Figure 9b). This invariant chaotic set is obtained when choosing an initial condition on the diagonal $y_n = x_n$, then one obtains an invariant set in the phase plane given by :

$$(5)\qquad \begin{cases} y_{2k+1} = a_2(x_{2k+1} + Q(-x_{2k+1})) \\ y_{2k} = x_{2k}, \qquad k = 0,1,2,\ldots \end{cases}$$

## VI CONCLUSION

We have studied a DPCM transmission system with zero input. It has permitted to show intrinsic properties of the system. Chaotic phenomena can be obtained, as in the system with non zero input [3][4]. PSD have been plotted, putting in evidence that far from bifurcations [5], chaotic signals can have interesting spectra, useful for applications.

## References


[1] C.Uhl - D.Fournier-Prunaret – « Chaotic phenomena in an order 1 DPCM transmission system ». *International Journal of Bifurcation and Chaos in Applied Sciences and Engineering, vol.5, n° 4, août 95, pp.1033-1070.*

[2] C. Mira, L. Gardini, A. Barugola, J.C. Cathala, « Chaotic dynamics in two-dimensional noninvertible maps », *World Scientific*, Series A, Vol. 20, 636 pages, juin 1996.

[3] D. Fournier-Prunaret, « Some complex situations in a (Z1, Z3, Z1) two-dimensional map », Proceed.*ECIT96*, Urbino (Italie), 8-14 septembre 1996.

[4] D. Fournier-Prunaret – « Chaotic attractors in transmission system », *NOLTA'98*, 14-17 septembre 1998, Crans-Montana, Suisse, Proceed. Vol. 2, pp 735-738.

[5] V. Guglielmi, D. Fournier-Prunaret, G. Kolumban & Z. Jako, "Composantes spectrales du chaos", *Gretsi 2001*, Toulouse (France), September 2001.

[6] L.Gardini - D. Fournier-Prunaret - C.Mira – « Some contact bifurcations in two-dimensional examples ». *Grazer Math. Ber., n°334, 1997, p77-96.*


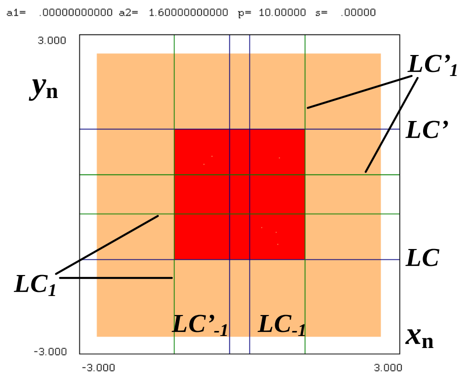


**Figure 9a**: The grey square is an absorbing set for $p$ = 10 and $a_1$ = 0.

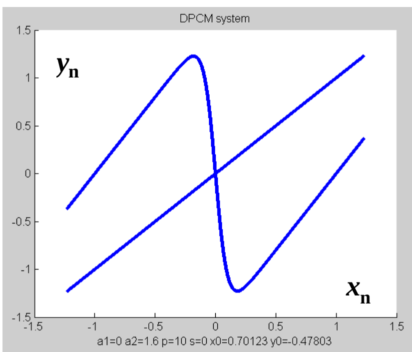


**Figure 9b**: An invariant chaotic set with zero Lebesgue measure inside the square of Fig. 9a when $p$ = 10 and $a_1$ = 0.

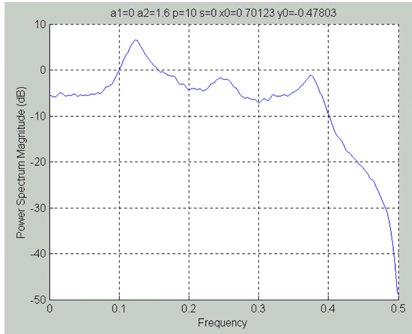


**Figure 9c**: PSD of the chaotic set of Figure 9b. Small peaks appear at frequency 1/8, 2/8, 3/8.

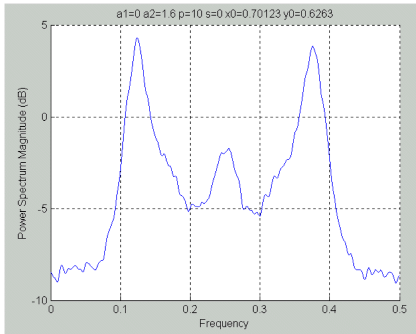


**Figure 9d**: PSD of the square chaotic attractor of Figure 9a. Periodic components appear, always due to a period doubling bifurcation cascade. One can notice high peaks at frequency 1/8, 2/8, 3/8.

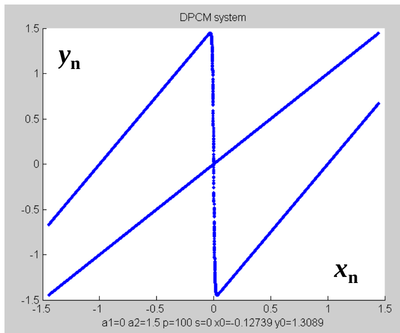


**Figure 10a**: The chaotic set with zero Lebesgue measure when $p$ = 100 and $a_1$ = 0.

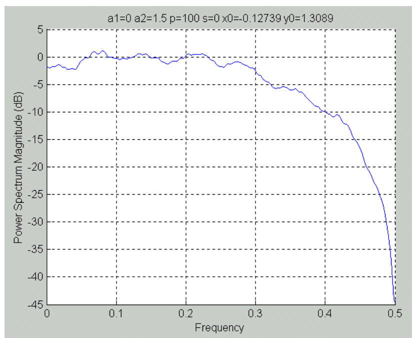


**Figure 10b**: PSD of the chaotic set of Figure 10a. No periodic component appear.